

Studying the Ursa Major Supercluster of Galaxies

© F.G. Kopylova^{1,2}, A.I. Kopylov^{1,3}

¹ Special Astrophysical Observatory,
Nizhnii Arkhyz, Karachai-Cherkessian Republic, 369167, Russia

² Email: flera@sao.ru, ³ Email: akop@sao.ru

Abstract: Based on SDSS (Sloan Digital Sky Survey) and 2MASS (Two Micron All Sky Survey) data, we have investigated the structure of the Ursa Major (UMa) supercluster, near IR properties and peculiar motions in the system and its nearest neighbourhood. Three large filamentary structures (layers), with redshift ranges 0.045-0.055, 0.055-0.065, and 0.065-0.075, are identified in the supercluster. These layers are stretched along right ascension, do not overlap in the plane of the sky and contains almost all clusters that are identified in the UMa system (12 clusters). The infrared luminosities (total K-band light) of the clusters of galaxies, the M/L_K ratios and total number of cluster members within radius R_{200} correlate with their masses (luminosities) closely following the relations derived previously for a large sample of clusters and groups of galaxies. The total scatter in the relations for UMa clusters are about a factor 2 smaller than for field clusters. This fact may indicate that field clusters are dynamically younger.

To determine the dynamical state of the UMa system we have compiled a sample of early-type galaxies with a measured velocity dispersion in SDSS DR4. Using the Fundamental plane of the early-type galaxies, we determined the distances and found the peculiar velocities of the early-type galaxies and clusters of galaxies in the supercluster reference frame. The deviations from the Hubble law in the UMa system consisting of three filamentary structures point tentatively to a mutual approach of these three subsystems - the UMa system begins to deviate from the overall Hubble expansion. On the whole, the pattern of peculiar velocities inside the supercluster is consistent with the observed overdensity.

1. Introduction

The superclusters of galaxies, the largest systems in the Universe, are giant filamentary structures in the large-scale structure or sheet-like structures, which surround large underdense regions criss-crossed by a variety of filamentary structures (e.g., such superclusters as Perseus [1] and Pisces-Cetus [2]) and are not virialized structures. General properties of superclusters of galaxies found in of the 2dFGRS and SDSS are investigated by Einasto et al. [3],[4],[5]. Properties of galaxies and clusters in the supercluster environment (Shapley) are studied by Padone et al. [6], Proust et al. [7], Mercurio et al. [8]. The peculiar motions in the region of various superclusters are investigated by (Aaronson et al. [9] in the Hydra-Centaurus supercluster and by Han and Mould [10], Baffa et al. [11], Hudson et al. [12] and Springob et al. [13] in the Perseus-Pisces supercluster). Investigation of the dynamical state of two large superclusters, Shapley [14] and Corona Borealis [15,16], suggests that their central regions are at the stage of gravitational collapse. The shape and structure of superclusters in Λ CDM concordance cosmology are determined in [17].

The UMa supercluster is an isolated one and is of interest in studying the composition of the system and the evolution of its constituent elements (galaxies, filaments, and clusters of galaxies) as well as the dynamical state of the system as a whole, which characterizes the mass distribution on a supercluster scales. The measured radial velocities of galaxies (more than 2000 within the supercluster) make it possible to study the large-scale structure in the system. From these data we found the supercluster is a large flattened structure with sizes of 40 x 15 x 125 Mpc in right ascension, declination, and line of sight, respectively and is divided along the line of sight into three filamentary subsystems (layers) (Fig. 1). We found the overdensity of the UMa system in its central part ($\alpha = 11^{\text{h}}12^{\text{m}}-12^{\text{h}}07^{\text{m}}$, $\delta = 53^{\circ}35'-56^{\circ}45'$, $0.045 < z < 0.075$) compared to the surrounding region with a size of about 150 Mpc (the cosmological parameters $\Omega_m=0.3$, $\Omega_\lambda=0.7$, $H_0=70$ km/s/Mpc are used throughout this paper) from galaxies with redshifts (according to NED data; these are mainly SDSS DR4 data) to be ≈ 3 by the galaxy number and ~ 15 by the Abell cluster number [18] together with additional clusters (according to NED data) discovered in X-rays. This overdensity is high enough for the system to be gravitationally bound, for example, for the spherical case [19].

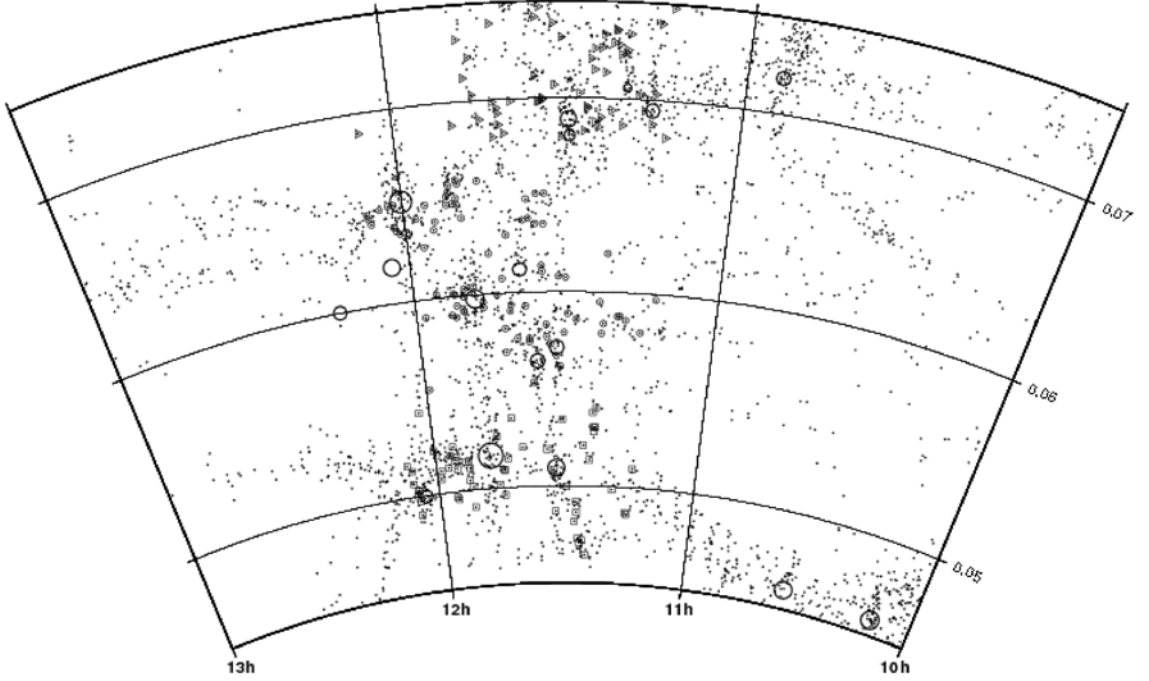


Figure 1. Distribution of galaxies on the right ascension - redshift plane in the central part of the supercluster and its neighbourhood in the declination layer $\delta=53^{\circ}35'-56^{\circ}45'$. The clusters of galaxies in the layer $\delta=50^{\circ}-60^{\circ}$ are indicated by the large circles with radii proportional to R_{200} . The early-type galaxies belonging to the three UMA subsystems are highlighted by the squares (I), circles (II), and triangles (III).

2. Relation between the IR Luminosity and Mass of Cluster

The main advantages of infrared (IR) photometric studies is their relative insensitivity to dust and to the last starburst; therefore, the stellar masses of the galaxies are traced better. Line-of-sight velocity dispersions of clusters were used to calculate the radius at which the cluster mass density exceeds the critical density of the universe by a factor of 200 (R_{200}), and the mass contained within that radius ($M_{200}=M_{\text{vir}}$), by assuming the cluster had an isotropic velocity field [20]. To determine the total infrared luminosity ($L_{200,K}$) for the cluster we sum the luminosities of observed cluster galaxies within R_{200} and extrapolate cluster luminosity to the fixed absolute magnitude limit $M_K=-21^m$. We examine the correlations between the cluster mass and $L_{200,K}$, $M_{200}/L_{200,K}$, N_{200} (the total number of cluster members) for dynamical radius R_{200} . We find the following relations:

a) for 10 UMA clusters (A1270, A1291A, A1318, A1377, A1383, A1436, Anon1, Anon3, Anon4, Sh166): $L_{200,K} \propto M_{200}^{0.71 \pm 0.08}$, $M_{200}/L_{200,K} \propto M_{200}^{0.29 \pm 0.08}$, $N_{200} \propto M_{200}^{0.71 \pm 0.08}$;

b) for 11 field clusters (A1003, A1169, A1452, A1461, A1507, A1534, RXCJ1010.2+5429, RXJ1033.8+5703, RXCJ1053.7+5450, RXCJ1122.2+6712):

$L_{200,K} \propto M_{200}^{0.59 \pm 0.12}$, $M_{200}/L_{200,K} \propto M_{200}^{0.41 \pm 0.12}$, $N_{200} \propto M_{200}^{0.62 \pm 0.12}$.

The *rms* scatter in the relations for UMA clusters (20%) is about a factor 2 smaller than for field clusters (44%). Figure 2 shows $L_{200,K}$ versus M_{200} for the UMA and field clusters. Our preliminary results are published in Kopylov and Kopylova [21].

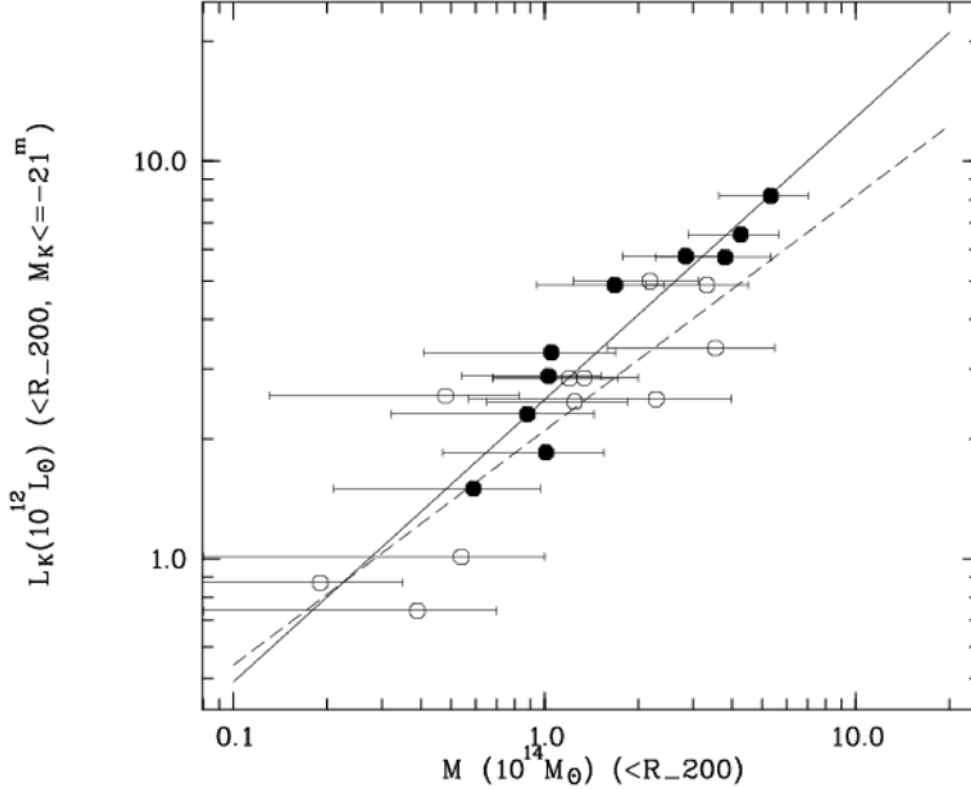


Figure 2. Plot of $L_{200,K}$ versus M_{200} for UMa clusters (filled circles) and field clusters (open circles). The solid (UMa) and dashed (field) lines are the best-fit relations.

3. Peculiar motions in the UMa Supercluster region

The Hubble law ($cz = H_0 r$) makes it possible to determine the distance to a galaxy in the first approximation by ignoring the peculiar velocity of the object. Measuring the distance (r) by a different method, we can separate an additional component (along the line of sight), the peculiar velocity of a galaxy or a cluster of galaxies, from the directly observed radial velocity (cz): $V_p = cz - H_0 r$. To determine distances we used the Fundamental plane of early-type galaxies [22]. The fourth edition of the SDSS DR4 catalog [23] allowed us to compile a sample of early-type galaxies in the supercluster region ($7^{0.9} \times 3^{0.2}$) in the r filter. The galaxies were selected according to the following criteria: $\text{fracDeV}_r > 0.8$ (the parameter characterizes the contribution from the de Vaucouleurs bulge to the galaxy surface brightness profile), $\sigma > 100$ km/s, $e\text{Class} < 0$ (the parameter characterizes the galaxy spectrum - there are no detectable emission lines in the spectrum), and $r_{90}/r_{50} > 2.6$ (the concentration index is equal to the ratio of the radii within which 90% and 50% of the Petrosian fluxes are contained). We selected 153 galaxies in virialized regions of UMa clusters and 80 galaxies in virialized regions clusters surrounding the supercluster. Also we selected 58 early-type galaxies ($0.045 < z < 0.055$) in layer I; their mean z is 0.051. Layer II contains 83 galaxies ($0.055 < z < 0.066$) with a mean $z = 0.061$ and layer III contains 57 galaxies ($0.066 < z < 0.075$) with a mean $z = 0.071$ [24]. Figure 1 shows the distribution of galaxies belonging to these structures in the plane of the supercluster

We estimate the individual peculiar velocities of the clusters are, on average, low; they do not exceed the measurement errors by more than a factor of 1.5-2 (Fig. 3). The error in the distances to the clusters of galaxies (the mean for all clusters) is 6%. The peculiar velocities of the three filamentary structures as a whole that constitute the UMa supercluster are presented in Table 1. The peculiar velocities found are low and comparable to the measurement errors. The following main conclusion can be reached: the UMa system begins to deviate from the overall Hubble expansion (along the line of sight). At least the signs of the peculiar velocities of the filamentary structures suggest that there is already a tendency for this deviation.

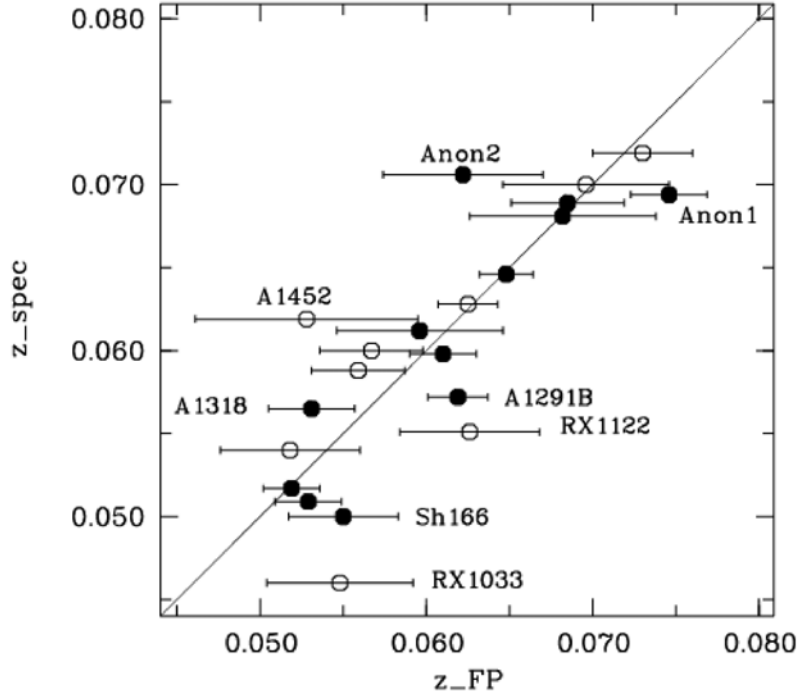


Figure 3. Hubble diagram for the UMa supercluster (filled circles). The clusters surrounding UMa are marked by the open circles. The *rms* errors of the distances are indicated. The names of the clusters with peculiar velocities exceeding 1σ are given.

Table 1. Peculiar velocities of layers (filaments)

Filament	N_{FP}	z_{spec}	z_{FP}	$\langle V_p \rangle$, km/s
I	58	0.05078	0.04906	+490±350
II	83	0.06107	0.06037	+200±360
III	57	0.07098	0.07181	-230±520

On the whole, the pattern of peculiar velocities inside UMa is consistent with the observed overdensity. For a spherical mass concentration at a linear stage of collapse, the radial peculiar velocity is defined by the equation [25] $V_p = 1/3 H_0 r \Omega^{0.6\delta} (1+\delta)^{-1/4}$. At $\delta = 3$ and $H_0 r = 3000$ km/s, we obtain $V_p \sim 1000$ km/s. However, since the UMa supercluster is highly elongated along the line of sight, the peculiar velocity along its major axis should be lower than that for a spherical mass distribution. According to our data (Table 1), the radial velocities of the two extreme layers (filaments) relative to the central layer are 300-400 km/s, which is consistent with the theoretical estimate, given the low measurement accuracy. The overdensity in the layers (filaments) is higher than that in the supercluster as a whole (Fig. 1). Therefore, one might expect the peculiar velocities to be higher inside the filaments.

4. Conclusions

The UMa supercluster comprises (according to the radial velocity measurements of galaxies in SDSS) three large filamentary structures that are clearly distinguishable both in projection onto the plane of the sky and from radial velocity measurements. We compiled a sample of early-type galaxies in the

central parts of 12 clusters of galaxies and in the filamentary structures constituting the UMa system as well as in the nine nearest clusters of galaxies in the UMa neighbourhood. Using the fundamental plane of the early-type galaxies, we determined the distances and found the peculiar velocities of the clusters of galaxies in the comoving reference frame associated with the supercluster as a whole independently of the radial velocity measurements for galaxies. For studying the relation between the dynamical mass and luminous matter in those clusters we determined the cluster masses within radius R_{200} and total K-band luminosities using the composite luminosity function of the clusters.

Our main results are the following.

(1) The peculiar velocities in the UMa system are low. They do not exceed the measurement errors by more than a factor of 1.5-2 and correspond in order of magnitude to the observed overdensity in the central part of the supercluster relative to the mean density in the surrounding volume 150 Mpc in size (about 3 by the galaxy number and 15 by the cluster number).

(2) The deviations from the Hubble law in the UMa system consisting of three filamentary structures (which are clearly distinguishable both from radial velocity measurements and in the plane of the sky) are insignificant, but they point to an approach of the filaments. To confirm the possible approach of the three UMa subsystems, the measurement accuracy must be increased by a factor of 2-3.

(3) The infrared luminosities $L_{200,K}$, the $M_{200}/L_{200,K}$ and N_{200} of the clusters in the supercluster region increases with mass, and the slopes of these relations are in agreement (within the errors) with the slopes derived by Lin et al. [26] for a large sample of X-ray clusters.

Acknowledgments

This research was supported in part by the Russian Foundation for Basic Research (grant 07-02-01417a). This publication makes use of data products from the Two Micron All Sky Survey, which is a joint project of the University of Massachusetts and the Infrared Processing and Analysis Center, funded by NASA and the National Science Foundation. This research has made use of the NASA/IPAC Extragalactic Database (NED). The creation and distribution of the SDSS Archive has been funded by the Alfred P. Sloan Foundation, the Participating Institutions, the National Aeronautics and Space Administration, the National Science Foundation, the US Department of Energy, the Japanese Monbukagakusho, and the Max Planck Society. The SDSS Web site is <http://www.sdss.org/>.

References

1. Gregory S.A., Tiftt W.G., Moody J.W., et al // AJ, 119, 567 (2000).
2. Porter S.C. and Raychaudhury S. // MNRAS, 364, 1387 (2005).
3. Einasto J., Einasto M., Saar E., et al // A&A, 459, L1 (2006).
4. Einasto J., Einasto M., Tago E., et al // A&A, 462, 811 (2007).
5. Einasto M., Einasto J., Tago E., et al // A&A, 464, 815 (2007).
6. Ragone C. J., Muriel H., Proust D., et al // A&A, 445, 819 (2006).
7. Proust D., Quintana H., Carrasco E. R., et al // A&A, 447, 133 (2006).
8. Mercurio A., Merluzzi P., Haines C. P., et al // MNRAS, 368, 109 (2006).
9. Aaronson M., Bothun G.D., Cornell M.E., et al // ApJ, 338, 654 (1989).
10. Han M. and Mould J. R. // ApJ, 396, 453 (1992).
11. Baffa C., Chincarini G., Henry R.B.C., and Manousoyanaki J. // A&A, 280, 20 (1993).
12. Hudson M.J., Lucey J.R., Smith R.J., et al // MNRAS, 291, 488 (1997).
13. Springob C.M., Haynes M.P., and Giovanelli R. // BAAS, 35, 1283 (2003).
14. Ettory S., Fabian A.C., and White D.A. // MNRAS, 289, 787 (1997).
15. Small T.A., Ma Ching-Pei, Sargent W.L.W., and Hamilton D. // ApJ, 492, 45 (1998).
16. Kopylova F.G. and Kopylov A.I. // Astron. Lett., 24, 491 (1998).
17. Wray J. J., Bahcall N. A., Bode P., et al // ApJ, 652, 907 (2006).
18. Abell G.O., Corwin H.G. and Olowin R.P. // ApJS, 70, 1 (1989).
19. Dünner R., Araya P.A., A. Meza A., and Reizenegger A. // MNRAS, 366, 803 (2006)
20. Carlberg R.G., Yee H.K.C., Ellingson E., et al // ApJ, 485, L13 (1997).
21. Kopylova F.G. and Kopylov A.I. // Astron. Lett., 32, 84 (2006).
22. Adelman-McCarthy J.K., Aqueros M.A., Alam S.S., et al // ApJS, 162, 38 (2006).
23. Kopylova F.G. and Kopylov A.I. // Astron. Lett., 33, 211 (2007).
24. Bernardi M., Sheth R.K., Annis J., et al // AJ, 125, 1866 (2003).
25. Yahil A. The Virgo Cluster of Galaxies, Ed. by O. Richter and B. Binggeli (ESO, Garching, 1985), p.359.
26. Lin Y.-T., Mohr J.J., and Stanford S.A. // ApJ, 610, 745 (2004).

